

INTEGRATING CRYOGENIC TANKS MODEL IN HYDROGEN AIRCRAFT DESIGN FOR PARAMETRIC PERFORMANCE ANALYSIS

R. Parello^{1,2}, S. Defoort¹, E. Benard² & Y. Gourinat²

 1 ONERA , 2 Av. Edouard Belin , Toulouse, France 2 ISAE-SUPAERO, 10 Av. Edouard Belin , Toulouse, France

Abstract

In response to the climate crisis, the aviation industry pledged through ICAO to become climate neutral by 2050. A promising solution to achieve this goal is the introduction of hydrogen-fueled aircraft, as they could emit no greenhouse gases in flight. Using hydrogen as fuel on an aircraft presents however huge challenges, especially due to its complex storage, as it must be stored in pressurized cryogenic tank. This study focuses on the integration of a medium-fidelity cryogenic hydrogen tank model into an overall aircraft design tool (FAST-OAD) and its exploitation to conduct several parametric studies on a medium-range, tube- and wing hydrogen aircraft. Results show a wide range of tank and aircraft performance, justifying the need for a hydrogen tank model in conceptual design. A strong dependency of aircraft performance on fuselage radius is highlighted, although not due to the hydrogen tank. The maximum design pressure of the tank is the second most important parameter for aircraft performance, suggesting tanks with a low design pressure differential. The increased amount of hydrogen that would need to be vented can be favorably offset by using thicker insulation, with a zero-venting design remaining feasible. A trade-off analysis between integral and non-integral tanks was also made, and it shows a small advantage to the integral configuration. With the best-identified configuration, the energy consumption of hydrogen aircraft appears to be a few percent above that of conventional aircraft at iso-technology level.

Keywords: Aircraft Design, Hydrogen Tank, Conceptual Design, Multidisciplinary Analysis, MDA, Model, Parametric study, Configuration

1. Introduction

The worrying prospect of current climate change prompted countries around the globe to sign the Paris Agreement in 2015, which aims to limit the temperature increase on earth to 2°C by 2100. The challenge is to rapidly cut greenhouse gas emissions in the next few decades to reach global carbon neutrality by 2050, as the Intergovernmental Panel on Climate Change has demonstrated that there are the main cause of current global warming[1]. The aviation industry also announced through the International Civil Aviation Organization (ICAO) in 2022 that it will reach climate neutrality by the midcentury, when it is currently responsible for 5-6 % of the radiative forcing on earth (including non-CO2 effect)[2]. If sustainable aviation fuel (SAF) could reduce aircraft carbon emissions in the short-medium term, it is likely that it will not be sufficient to reach net zero as SAF availability will be limited and it doesn't solve the non-CO2 impacts. Another promising but challenging solution is therefore the introduction of carbon-free fuels, like hydrogen. Hydrogen combustion or hydrogen fuel cells don't emit carbon, so hydrogen-powered aircraft would fly carbon-free. If hydrogen can be produced in a sustainable way, aircraft life-cycle emissions would be really low, especially as studies have shown promising possibilities to reduce NOx emissions and mitigate contrails' impact of hydrogen turbines [3][4].

A hydrogen-fueled aircraft represents a very disruptive concept from conventional airliner. If some prototypes have already flown in the past, none have already been fully designed, built, or certified,

and they would require a profound change in airports and air traffic ecosystems. This concept also requires a profound revision of classical design and certification methods. Brewer summarized in [5] all the knowledge available at his time at NASA over hydrogen aircraft and he was one of the first to build models for a commercial, tube- and wing, hydrogen-powered aircraft. Since then numerous studies tried to design and assess the performance of very innovative concept. The European cryoplane study [6] showed for example in 2003 that this solution should be technically viable, although lots of further research and development were required. More recent research funded by the European Union confirmed the potential of hydrogen for air transport. [7]. Verstraete used Brewer's work as the basis for his long-range aircraft model. Cipolla et al. [8] and Palaia et al. [9] investigated the retrofitting of the european box-wing short-medium-range aircraft project PARSIFAL into an hydrogen aircraft. Van Woensel[10] designed a hydrogen version of the Flying V. Quiben et al. [11] developed an aircraft sizing tool called MOTIVATION to retrofit an A320 into a hydrogen aircraft. Prewitz et al. [12] estimated the performance of a regional hydrogen aircraft similar to the ATR-72. Maniaci [13] compared the energy consumption of hydrogen and kerosene aircraft. Most of those studies concluded that hydrogen aircraft have the potential to reduce the climate impact of air travel, but they highlighted the technical and economic challenges that they represent.

If hydrogen aircraft are so difficult to design, it is mainly due to the storage of hydrogen onboard. Hydrogen gas has indeed a very low energy density at standard temperature and pressure. Except maybe for regional flight, which is not the focus of this study, it must then be stored in liquid form at 20K to reach an acceptable energy density, which is still four times lower than kerosene. Hydrogen tank must therefore be cryogenic and pressurized and will require a large space, meaning it will represent a non-negligible weight. Tank design becomes then critical for aircraft performance, as demonstrated by Adler and Martins in [14] where they showed with the Breguet range equation that the energy consumption of a hydrogen aircraft increased exponentially when the tank gravimetric index 1 fell below 50%. Huete et al. confirmed this fact [15] by showing how the deliverable range for a wide-body aircraft almost doubles when the gravimetric index increases from 0.3 to 0.85. In their sensitivity analysis on the performance of a wide-body hydrogen aircraft, Jagtap et al. [16] also determined that for current technology, the gravimetric index should be at least 0.52 to match the concurrent kerosene aircraft range.

$$\eta_{grav} = \frac{m_{H2}}{m_{H2} + m_{tank}} \tag{1}$$

Hydrogen tanks are the result of compromises between safety requirements, ease of integration into the airframe, and thermal and structural performance, so a large variety of design configurations exist. To estimate the feasibility or performance of a hydrogen aircraft during conceptual design, it is then necessary to model those different solutions at this stage and compare them as studies disagree on the best solution. A cryogenic tank model is made of two part: a structural sizing model and a thermodynamic model to evaluate how much hydrogen is lost due to boil-off, i.e hydrogen changing state from liquid to gas. Verstraete's tank thermodynamic model[17] is the base on which many authors built their own hydrogen cryogenic tank model, like Winnefeld et al. [18] who compared different hydrogen tank geometries, Van Woensel [10] in the flying V, Sekaran et al. [19] who looked at a hydrogen-powered turbo-electric distributed propulsion concept, or Gomez and Smith [20] who sized an hydrogen tank for medium-range civil aircraft. This model assumes a steady state and a homogeneous state inside the tank to determine the hydrogen lost in boil-off due to incoming heat leakage. A few studies, like [21] tried however to use a more detailed approach inspired by what can be done in the space launcher industry [22]. For the structural design, both Verstraete and Brewer studied mainly the integral concept, where the fuselage is also the tank wall because it should reduce the aircraft's empty weight. Brewer considers a stiffening structure for his tanks that is sized according to certification constraints in terms of limit and ultimate load. His methodology, like the one from Gomez et al. [20] for structural design is, however, based on finite-element and designspecific. The lack of generic capabilities and the high fidelity level complicate its use in conceptual design. Verstraete only sized the tank wall for the pressure differential and didn't consider a stiffening structure. Like most of the previously cited authors, Winnefeld and al. adopt a similar methodology in their non-integral tank study [18] but include elliptical tank design capabilities. Their simulation concluded that elliptical tanks have a significant structure weight penalty, degrading tank efficiency

as the structure represents at least 70% of tank empty mass. They also found a decrease in storage density when fuel is split into several smaller tanks. Onorato et al. [23] built a hydrogen aircraft multidisciplinary design analysis framework also based on Verstraete tank thermodynamic and structural models. They used this framework to compare multiple tank configurations and confirmed that an integral tank is indeed more efficient, especially at longer ranges, or that larger fuselages tend to decrease aircraft efficiency. They stressed, however, that the optimal tank configuration depends on the aircraft category, justifying the need for a parametric and adaptive sizing framework. To fully explore all possible designs however, it must be relatively quick to run in order to be integrated into an iterative optimization process.

The purpose of the present work is to use a new higher-fidelity thermodynamic [24] and structural model [25] of an aircraft's hydrogen tank into FAST-OAD [26], which is an overall aircraft design tool. The new thermodynamic tank model doesn't consider the tank to be homogeneous but composed of three control volumes that exchange mass and energy. The structural model is able to size the tank wall and the stiffening structure for both integral and non-integral tank. This is done by following the current certification constraints of the CS-25 relative to pressurized cylinders [27]. The generic sizing tool created allows the study of various tank configurations and technologies. Parametric studies are conducted to evaluate the sensitivity of aircraft or tank efficiency to tank design variables. The structure of this paper will first describe this new model and how it was implemented in FAST-OAD. Several parametric studies and design of experiments on hydrogen tank configurations will then be presented to highlight and quantify hydrogen aircraft performance dependency on tank or mission parameters.

2. Methodology

2.1 FAST-OAD : an Aircraft Design Tool

Aircraft design is a complex process as it involves multiple disciplines (aerodynamics, structure, controls, etc.) that are coupled because some disciplines depend on other discipline output. The basic example is the structure-aerodynamic coupling: aerodynamic loads on the wing depend on its shape, while those loads deform the structure of the wing, thus changing the shape of the wing and so the associated aerodynamic loads. This interdependence can be represented in an eXtended Design Structure Matrix (XDSM) diagram, as in figure 1.

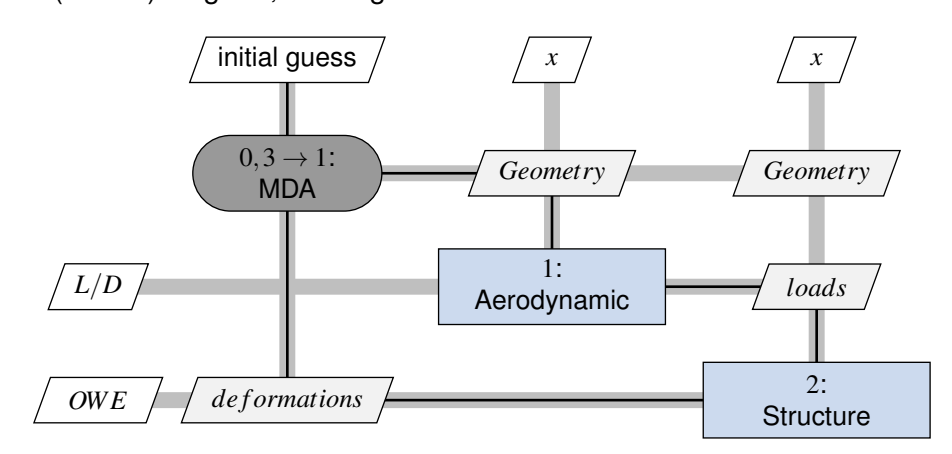


Figure 1 – Illustration of the aerodynamic-structure discipline coupling in aircraft design within an XDSM graph

To solve this coupling problem and lots of others present in aircraft design, the multidisciplinary design analysis and optimization (MDAO) paradigm have emerged sin the end of the 90s. The idea with MDAO is to solve an analysis with multiple coupled disciples in an iterative and automated process. This was implemented for aircraft design by ONERA and ISAE-SUPAERO in FAST-OAD (Future Aircraft Sizing Tool Overall Aircraft Design) [26]. In its current version, FAST-OAD loops the multidisciplinary analysis around the aircraft block fuel mass. It computes indeed the fuel mass required for the mission based on an initial maximum take off weight (MTOW) guess and sizes the structure based on this fuel mass and the Top Level Aircraft Requirements (TLARs). It can then determine the

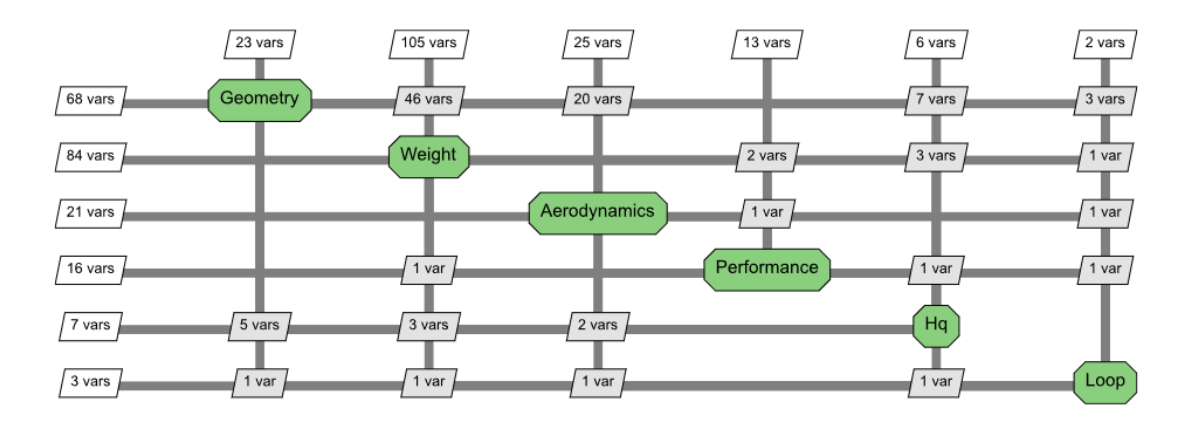


Figure 2 – FAST-OAD multidisciplinary Analysis process [26]

TLAR	Value	Unit	Aircraft characteristics Value	Unit
		Offic	MTOW 101	tons
Passenger	239			tons
Payload	25	tons		
Cabin layout	3 x 3		OWE 54.5	tons
•			Block fuel 21.9	tons
Design range	2500	NM	Max L/D 17.4	
Cruise altitude	33 000	ft		2
	0.78	mach	Wing surface 138	m^2
Cruise speed		macm	Maximum Thrust 173	kN
Thrust-to-weight ratio	0.35			
Aspect ratio	9.9		Fuselage length 45.5	m
7 topost ratio	0.0		Wingspan 37	m

Table 1 – Reference kerosene aircraft characteristics

updated MTOW of this aircraft as it knows the structure's mass. It can finally recompute the updated fuel mass with a time-step integration of the mission profile and restart the process until the fuel mass and aircraft mass converges on a feasible aircraft design. The MDA process is represented on figure 2.

To ease the MDA process, FAST-OAD was implemented in Python under the OpenMDAO format developed by NASA [28] which was specifically tailored for this type of problem.

FAST-OAD was developed originally for conventional Tube and Wing (T&W) small to medium range aircraft. The models used in the various disciplines are mainly analytical and based on typical aircraft design literature or are in-house models. The FAST-OAD also incorporates a low-fidelity aerodynamic model for low-speed aerodynamics during take-off and landing, a "rubber" engine model [29], as well as a quasi-static method for mission analysis. The code has been validated against the specifications of an Airbus A321 [30]. A reference kerosene aircraft has been created, whose design mission and main characteristics are presented in Table 1.

However, to be able to design hydrogen aircraft, some modules of the program had to be modified:

• Propulsion module: Several conventional aircraft have already been converted to hydrogen (for example the US successfully modified a B-57 to fly on liquid hydrogen [31] in the 1960's). This suggests that a hydrogen turbine won't differ that much from a conventional gas turbine. At the conceptual design level and for a first approach, it was considered acceptable to represent hydrogen turbines in FAST-OAD with the same rubber engine as conventional ones. The consumed fuel flow was just modified with respect to the ratio of specific energy between hydrogen and kerosene. By taking also into consideration the improvement in fuel consumption of new engines currently in production, the specific fuel consumption was reduced by a factor of 3.28 compared to a CFM-56 like engine.

Component	Mass (kg)
Fuel lines	200
Venting system	150
Refuel-Defuel system	300
Pressurization system	50

Table 2 – Mass of cryosystems included in the design, adapted from Brewer [5]

• Geometry module: The geometry module defines the geometry of all aircraft components based on their masses and a few empiric rules. This module was modified to determine the tank geometry depending on block fuel. The choice was made in this study to always place the tank(s) behind the cabin for safety reasons. Placing it in front of the cabin would indeed prevent access to the cockpit during flight and might compromise passenger safety in the event of a crash. If those concerns turn out to be unfounded in the future, the tank could then be easily placed anywhere along the fuselage.

The tanks considered are cylindrical tanks with hemispherical or elliptical bulkheads. The geometry module first computes the fuel volume with the block fuel mass and liquid hydrogen density, which depends on liquid hydrogen initial temperature. To avoid rapid variation in tank pressure in the case of fuel withdrawal or fuel expansion due to temperature elevation, a 3% margin in tank required volume is added. The tank's external diameter is equal to the fuselage diameter, which is determined by the cabin layout, so it becomes possible to estimate the required tank length, taking into account the tank's insulation and wall thickness and the volume available in each bulkhead, varying with their shape. The model also allows for the fuel to be divided into multiple tanks in the fuselage, in which case the distribution ratio must also be given. The tank length plus one meter dedicated to other cryogenic systems (pump, valve, refueling system, gauge, etc) is then added to the fuselage length.

- Weight module: In this discipline, the structural model presented in Section 2.2is added to determine the tank mass and center of gravity based on the previously defined geometry. This mass is added to the airframe mass. The mass of other cryogenic systems required for a hydrogen aircraft like pumps, valves, refueling systems or fuel lines, is taken from Brewer's estimations [5] and presented in table 2. However, as Brewer considered a double-deck long-range hydrogen aircraft with four separate tanks, the total weight for those systems was divided by two, considering the focus of this work is on medium-range aircraft with one or two tanks only.
- Handling quality module (HQ): while sizing the tank geometry, the center of gravity of the tank is also computed to be considered when assessing the stability and control of the aircraft.
- Performance module: In the original FAST-OAD design loop, the performance discipline evaluates the previously sized aircraft on its mission with a time-step integration. In the hydrogen adapted FAST-OAD, after this step where the consumption, velocity and altitude of the aircraft are determined at any given time, the mission is post-processed by the tank thermodynamic model presented in Section 2.3 This leads to an estimation of the amount of hydrogen boil-off, which is then added to the total block fuel.

2.2 Tank structure sizing

The structural model of the tank is an important part of tank design process, as the majority of the tank weight is indeed due to its structure. In addition to storing hydrogen, the tank structure serves at least two other goals: it must be able to hold a pressure differential between the interior and exterior of the tank and be able to endure bending, torsion, and shear loads transmitted by the fuselage. Even in the case of a non-integral tank, some of these loads will inevitably be transmitted by the supporting structure of the tank inside the airframe.

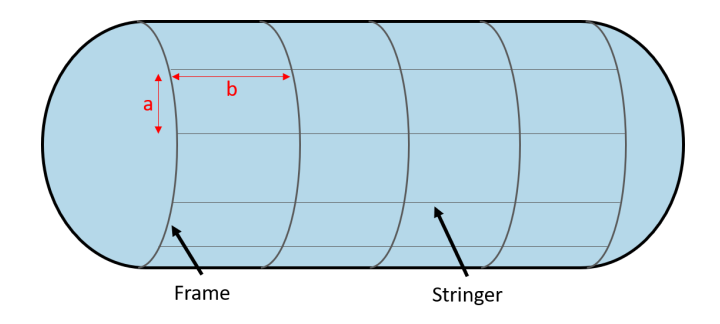


Figure 3 - Tank structure [25]

As the liquid hydrogen is stored at 20K, the tank internal pressure should always stay above the external pressure to avoid air or water leaking inside and freezing, clogging the fuel system. The hydrogen boil-off will, on the other hand, cause a gradual rise in pressure. The tank is therefore sized to withstand a maximum pressure differential with the exterior, above which the excess pressure will have to be vented. As the tank is situated in a non-pressurized part of the fuselage, the atmospheric pressure outside will vary with altitude. This means that the acceptable range for pressure inside the tank also depends on altitude. In the case of an integral tank concept, the structure is part of the fuselage and must, as a consequence, also support the different bending and shear loads of the fuselage. The methodology used to size the tank structure is, for the most part, the one described by the authors in [25]. A brief summary of the methodology and its latest evolution is presented in the following paragraph.

For a cylindrical-shaped tank, the structure can be divided into three main components visible in figure 3: the tank wall, the frames, and the stringers, the last two ones forming the stiffening structure. The stringers are longitudinal stiffeners, while the frames are circular ones. In the current CS-25, the role of each component of a pressurized cylinder, such as the tank or the fuselage, is very specific. Each has indeed different requirements[27]: the wall must withstand the operational load alone, which is the bending, shear, torsion, and pressure load encountered during a nominal mission. I.e., the wall must be thick enough to not suffer plastic deformation under those loads. To satisfy that constraint, the stress tensor 3 in the wall is computed and checked against a design criteria. The currently implemented model can use the classical Von Mises criteria, or a more innovative criteria based on principal strains presented in equation 2. This last criteria was originally built for composite materials, but it can be used for metallic structure as well.

$$-3*10^{-3} \le \varepsilon_{III} \le \varepsilon_{I} \le \varepsilon_{I} \le 4.5*10^{-3}$$
 (2)

The bending and shear loads transferred by the fuselage to the tank are computed with a simple beam model presented in [25]. To improve accuracy, the additional lift required to compensate for the downward force of the horizontal stabilizer is now taken into account.

$$\Sigma(\theta) = \begin{pmatrix} \frac{\Delta P_{OL} r_{tank}}{t_{skin}} & \sigma_{xy}(\theta) & 0\\ \sigma_{xy}(\theta) & \frac{\Delta P_{OL} r_{tank}}{2t_{skin}} - \frac{M_z sin(\theta)}{\pi t_{skin} r_{tank}^2} & 0\\ 0 & 0 & 0 \end{pmatrix}$$
(3)

The wall should also not buckle under the operational load. As the wall buckling depends on stringers and frame pitches (respectively a and b on figure 3), this criteria determines how many frames and stringers are needed on the tank.

Between the operational load and the ultimate load, defined as two times the operational load, the wall might buckle, so the super stiffening structure must be able to bear all the loads. The super stiffening structure is composed of the frame and stringer plus a small part of the wall around their attach point that should not buckle [32], as represented on figure 4. Frames and stringers' sections are then sized so that the super stiffeners remain below the break stress at the ultimate load but also remain in elastic deformation at the limit load, defined as the ultimate load divided by 1.5 (approximately 1.33)

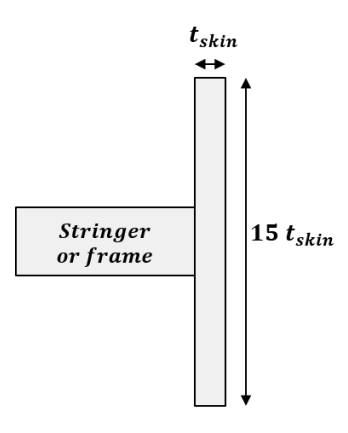


Figure 4 – Super stiffener representation [25]

times the operational load). This last sizing process was simplified as the formal optimization problem presented in [25] was deemed unnecessarily computation-intensive. It was replaced by the solving of equation 4 to determine the stringers section and of equation 5 for the frame section.

$$\sigma_{1,1(stringer)} = \frac{\Delta P \pi r^2}{N_{strg}(15w_t^2 + A_{strg})} - \frac{M_z sin(\theta)}{\pi r^2 (w_t + \frac{N_{strg} A_{strg}}{2\pi r})} \le \sigma_e$$

$$A_{strg}^2 \frac{N_{strg}}{2\pi r} + A_{strg} (w_t + \frac{15w_t^2 N_{strg}}{2\pi r} - \frac{\Delta P r}{2\sigma_e} + \frac{M_z sin(\theta)}{\pi r^2 \sigma_e}) + 15w_t^3 - \frac{\Delta P \pi r^2 w_t}{N_{strg} \sigma_e} + \frac{15M_z sin(\theta)w_t^2}{\pi r^2 \sigma_e} \ge 0 \qquad (4)$$

$$\sigma_{1,1(frames)} = \frac{\Delta P L_{tank} r}{N_{frame}(15w_t^2 + A_{frame})} \le \sigma_e$$

$$A_{frame} \ge \frac{\Delta P L_{tank} r}{N_{frame} \sigma_e} - 15w_t^2 \qquad (5)$$

Once the skin thickness and stiffeners sections are determined, it becomes possible to compute their volume and so their masses.

2.3 Tank thermal analysis

A liquid hydrogen tank is said to be cryogenic because it must keep the fuel at around 20K. Designing such a tank requires a detailed thermodynamic analysis to determine the required insulation and how the liquid hydrogen will evolve during the mission. The tank will indeed not stay at a constant temperature or pressure during the whole mission. The heat leaking inside the tank will cause hydrogen to boil off, which will increase the internal pressure. The tank is therefore in a a periodic cycle of self-pressurization and venting, where hydrogen is released in order to stay below the maximum design pressure for which the tank structure have been sized. The adopted thermodynamic model for both the self-pressurization and venting phases is similar to the detailed in a previous paper of the authors [24], with some improvements coming from recent discoveries. It will be summarized in the following paragraphs.

In the entire thermal model, the thermodynamic properties of chemical species are computed using the CoolProp Python library [33].

2.3.1 Thermal circuit model

The thermodynamic model of the tank is divided into three parts: the thermal circuit, which estimates how much heat is entering the tank; the boil-off model, which describes the evolution of the fuel in the tank in response to this heat inflow; and the venting phase, which occurs when the pressure reaches its maximum.

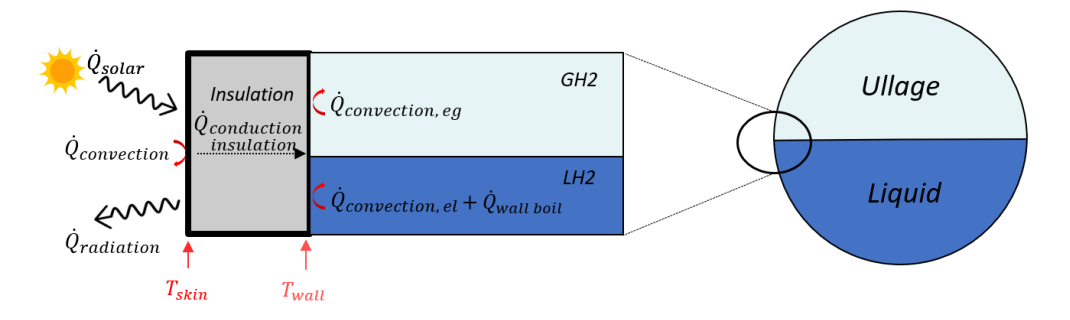


Figure 5 – Heat flows impacting a cryogenic hydrogen tank

The first part is called the thermal circuit model because it uses an analogy with electrical circuit, replacing electrical resistance with thermal resistance to determine the incoming heat flow. This methodology allows for a division in incoming heat flow into the tank between different physical phenomena. Each phenomenon is associated with its own heat flow, which is individually computed and then summed up. The model considers two surfaces that are assumed to always be in thermal equilibrium: the tank internal surface, the tank wall, and the tank external surface, called here the tank skin, which can also be the aircraft skin if the tank is integral.

For the tank skin, four heat flows represented on figure 5 can be considered [17], [34]:

• Convective heat flow : $\dot{Q}_{ext,conv}$

• Conductive heat flow through the insulation: \dot{Q}_{cond}

• Radiative heat flow towards the exterior environment: \dot{Q}_{rad}

• Solar irradiation: \dot{Q}_{solar}

For the internal wall of the tank, two phenomena should be taken into account:

• Natural convection on the internal wall: $\dot{Q}_{int,conv}$

• Conductive heat flow through the insulation: \dot{Q}_{cond}

The authors are aware that in cases where the wall temperature is above the saturation temperature, hydrogen should boil directly on the wall, affecting the convective heat flow and gas volume. The phenomenon is however highly non-linear and effort is still ongoing to incorporate it, but in the mean time the assumption that the convective heat flow is sufficient was made, as in the majority of previous studies.

With the thermal equilibrium assumption, T_{wall} can be obtained by solving the following system:

$$\begin{cases} \dot{Q}_{ext,conv} + \dot{Q}_{rad} - \dot{Q}_{solar} - \dot{Q}_{cond} = 0\\ \dot{Q}_{int,conv} - \dot{Q}_{boil} - \dot{Q}_{cond} = 0 \end{cases}$$
(6)

The system 6 is in fact solved several times, one for each "region" of the tank. Those regions are defined by their internal environment (gaseous or liquid hydrogen) and the external environment (aircraft interior or atmosphere, lit or not by the sun) they are in contact with. This yields multiple heat flows entering the gaseous or liquid hydrogen volumes. Those heat flows are then summed up to determine the total flow arriving in each phase.

2.3.2 Boil off model

Once the heat transfer to the liquid and gaseous hydrogen is known, it becomes possible to determine the evolution of both hydrogen phases. Unlike most previous studies, the model used here doesn't make the homogeneous tank assumption but considers three separate control volumes: bulk liquid hydrogen, gaseous hydrogen (also called the ullage), and the interface between both. The interface is an infinitely thin layer with a definite temperature but no mass, like Ramos in [35]. The state of these control volumes can be fully described with only four variables: T_g , T_l , m_g and V_g . By applying the conservation of energy law to each volume and at each time step, the system 7 is obtained. Here, a modification to the model developed in [24] can be observed with the addition of the term $V_l\beta_l\dot{T}_l$ in the time variation of the gaseous volume. This allows the thermal expansion of liquid hydrogen to be taken into account. If this term is neglected, the ullage volume tends to increase too slowly. Consequently, the liquid volume decreases too quickly, which leads to an artificial over-consumption (because the hydrogen in question disappears from the tank but is not in reality consumed by the engine). Due to the relatively high thermal expansion coefficient of liquid hydrogen, taking this phenomenon into consideration can represent a difference of several hundred kilograms of hydrogen on an entire mission (the density of liquid hydrogen decreased by 10% between 14K and 21K).

$$\begin{cases} \dot{m}_{g} = \frac{\dot{Q}_{gs} - \dot{Q}_{sl}}{h_{vap} + c_{p,l} (T_{s} - T_{l}) + (h_{g} - h_{sat})} + \dot{m}_{boil} + \dot{m}_{pressurization} \\ \dot{T}_{g} = \frac{\dot{Q}_{eg} - \dot{Q}_{gs} - P_{g} \dot{V}_{g} + \dot{m}_{g} h_{g} + h_{l} \dot{m}_{boil} - \dot{m}_{g} u_{g}}{m_{g} c_{v,g}} \\ \dot{V}_{g} = \frac{\dot{m}_{g} + \dot{m}_{f}}{\rho_{l}} - V_{l} \beta_{l} \dot{T}_{l} \\ \dot{T}_{l} = \frac{\dot{Q}_{el} + \dot{Q}_{sl} + P_{l} \dot{V}_{l} - \dot{m}_{g} h_{l} + h_{l} \dot{m}_{f} - \dot{m}_{l} u_{l}}{m_{l} c_{p,l}} \end{cases}$$

$$(7)$$

A representation of the model can be seen in figure 6

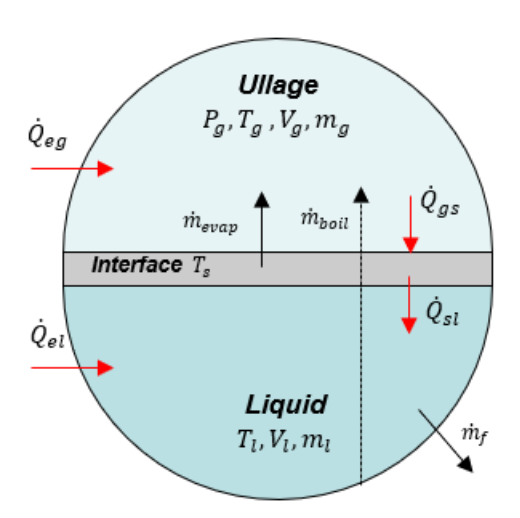


Figure 6 – Self-pressurizing hydrogen tank model [24]

2.3.3 Venting

The tank thermal model is integrated into FAST-OAD, where the user can define an initial tank pressure, temperature and fill level. With this and the mission profile computed in the performance module (including the altitude, velocity and consumption of the aircraft at each time step), it is possible to solve both systems 6 and 7 and estimate the evolution of the tank state during the mission. With the inevitable heat leakage into the tank, hydrogen boil-off caused an increase in pressure. Once the maximum pressure is reached, hydrogen must be vented. The venting phase is modeled as an instantaneous gas ejection, with an amount of gas released equal to what is necessary to make the pressure drop to the minimal pressure admissible in the the tank. The temperature of the ullage after venting was previously assumed to be equal to the saturation temperature in [24]. Investigations

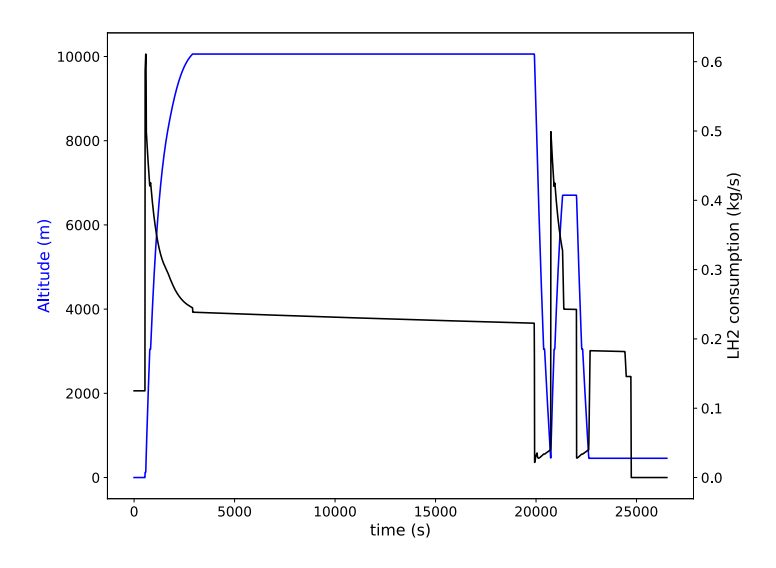


Figure 7 – Medium range aircraft design mission profile

showed that in some tank configurations this could lead to an ullage mass increasing during venting, which is physically impossible. The reason behind this phenomenon is that the temperature after venting doesn't drop to the saturation temperature. To determine the ullage mass lost during venting, the conservation of energy law is applied to the ullage:

$$\sum_{out} \dot{m}h = \frac{dE_{cv}}{dt}$$

$$\dot{m}_g h_g = \dot{m}_g u_g + m_g c_{v,g} \dot{T}_g$$
(8)

The ideal gas law can also be derived:

$$\dot{P}_g V_g = \frac{R}{M_{H2}} (\dot{m}_g T_g + \dot{T}_g m_g) \tag{9}$$

By combining the two previous equations, the derivative of the ullage mass becomes 10:

$$\dot{m}_g = \dot{P}_g V_g \frac{R}{M_{H2}} \frac{c_{v,g}}{c_{v,g} T_g + h_g - u_g} \tag{10}$$

As the variation of pressure during venting, equation 10 can be solved in one or several step to determine the new ullage mass (100 steps implemented in the model). The ideal gas law gives then the ullage temperature after venting.

3. Results

With the tank model now fully integrated into FAST-OAD, it becomes possible to design hydrogen aircraft and assess their performance and how they depend on tank configuration. The focus is here on a narrow-body aircraft with 240 passengers and a 2500 NM design range, which is similar to the A321 neo. Its design mission profile is represented in figure 7, along with the evolution of hydrogen consumption during the mission.

A first set of analysis was conducted to visualize how the tank design parameters impact the entire aircraft. To get a broad overview, it was decided to conduct a Design of Experiment (DOE) on some tank design parameters 3.1 This led to the identification of a few parametric studies of interest that are presented in Section 3.2

A few design choices were still fixed for this first study:

Table 3 – Tank model inputs

	Inputs	Value	Unit
Mission and Design	Passenger	239	
	Seat per row	6	
	Range	2500	NM
	Cruise altitude	33 000	ft
	Cruise speed	0.78	mach
	Dormancy time	30	min
	Thrust-to-weight ratio	0.35	
	Aspect ratio	9.9	
Tank initial State	Pressure	1.5e5	Pa
	Ullage temperature	25	K
	Fill level	97%	
Insulation	Thermal conductivity	0.026	$W.m^{-1}.K^{-1}$
(Polyurethane Foam)	Density	33	$kg.m^{-3}$
Tank material	Density	2825	kg.m ⁻³
(Aluminium 2026)	Poisson ratio	0.33	
	Young modulus	73.8	GPa
	Elastic limit stress	240	MPa
	Elastic break stress	420	MPa
	Thermal conductivity	230	$W.m^{-1}.K^{-1}$
	Tank skin infrared emittance	0.9	
	Tank sink solar absorptance	0.26	
Model time step		10	S

- the aircraft is equipped with only one hydrogen tank
- the tank is integral and placed behind the cabin
- The insulation is a polyurethane foam placed inside the tank
- · the tank structure is in aluminum

Table 3 summarizes the tank design inputs that were fixed.

3.1 Tank Design of Experiment

The design of experiment was carried out on the seven aircraft parameters presented in table 4. Those seven parameters are continuous variable that all affect the hydrogen tank. Max ΔP and min ΔP correspond to the maximum and minimum pressure differential between the tank interior and the external environment. The initial liquid temperature is the liquid hydrogen temperature at the start of the mission, while the insulation thickness is the thickness of the polyurethane foam insulating the tank. The fuselage width directly determines the tank diameter, as it is an integral tank. Finally, the shear and bending transmission ratios are introduced to assess how much the bending and shear load-bearing constraints affect the tank design. Here, a transmission ratio of 1 means the tank must withstand the full load present in the fuselage, while a ratio equal to 0.1 means that only 10% of the fuselage load is passed to the tank. Its structure can so be sized for a much reduced load.

A four hundred points DOE was built with the Latin Hypercube Sampling (LHS) method and the bound indicated in Table 4. For each DOE point, an aircraft was sized with the model presented previously in Section 2. Figure 8 represents for each design five key performance indicators or aircraft characteristics, where boil off is the amount of hydrogen that had to be vented due to boil off and tank-adjusted gravimetric index (GI) is defined in equation 11. This index takes into account the amount of hydrogen boil-off to differentiate tanks with good insulation, whereas the classical index could advantage tanks that are light due to poor insulation.

Table 4 - Tank inputs DOE

Inputs	lower	upper	Unit
max ΔP	0.8	4	bar
min ∆P	0.2	0.6	bar
Initial liquid temperature	15	21	K
Insulation thickness	0.02	0.2	m
Fuselage width	3.9	5.5	m
Shear load transmission ratio	0.1	1	
Bending load transmission ratio	0.1	1	

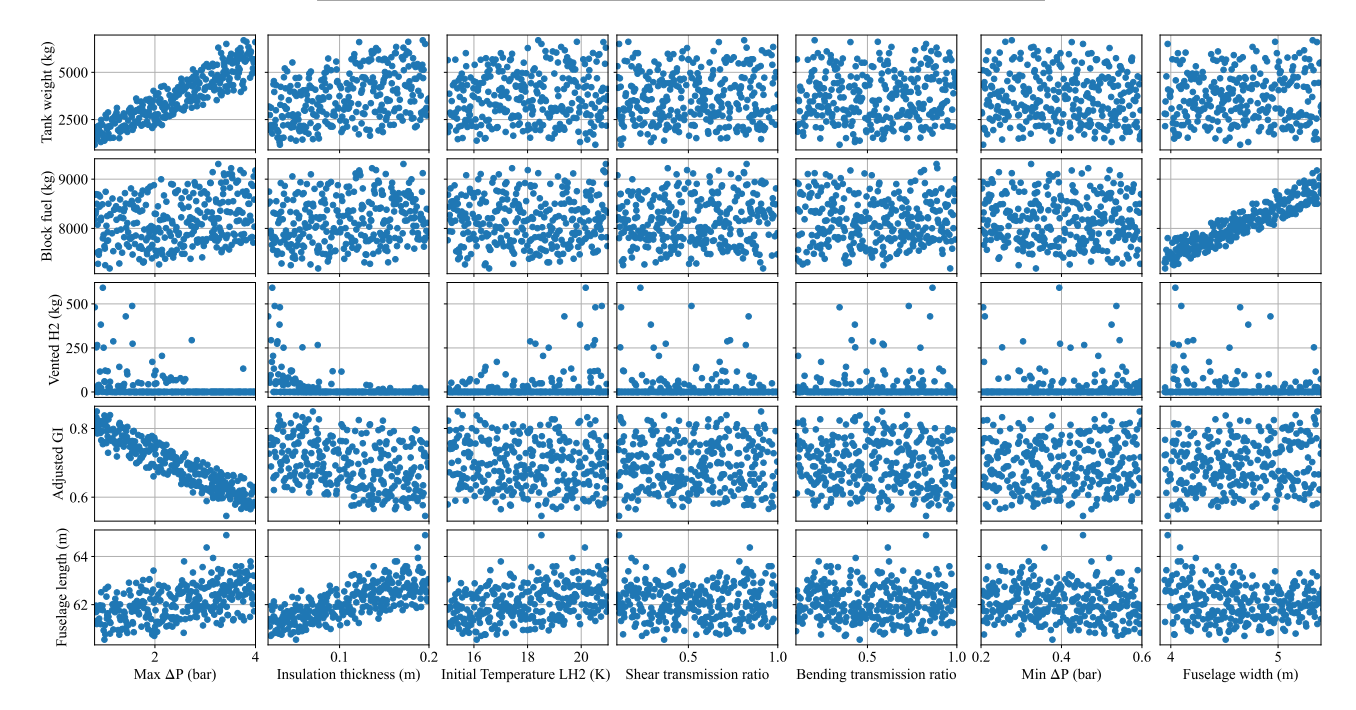
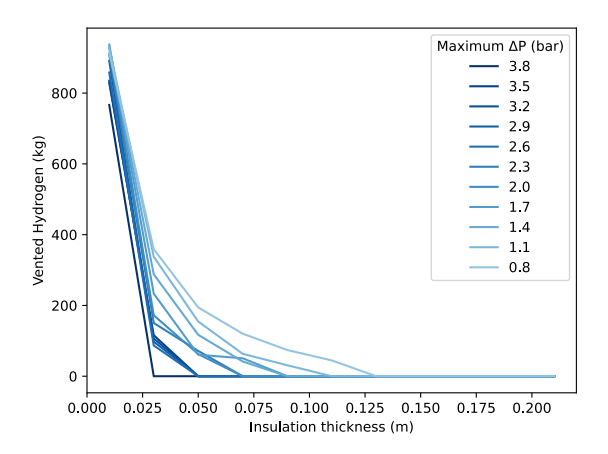


Figure 8 – Design of Experiment on tank design variables

$$\eta_{grav} = \frac{m_{H2} - m_{boil_off}}{m_{H2} + m_{tank}} \tag{11}$$

Several conclusion can be deduced from Figure 8:

- The adjusted gravimetric index ranges approximately from 0.55 to 0.85 across all the designs.
 This highlights the dependency of tank efficiency on design choices, justifying the inclusion of tank sizing in the aircraft preliminary design stage.
- The tank weight and efficiency seem most affected by the maximum design pressure differential, as points in the most left column are grouped along lines which indicates a strong correlation. An increase in the max ΔP can also significantly increase the length of the fuselage, probably because it increases the required block fuel mass, requiring a bigger tank. The amount of vented hydrogen however doesn't seem to depend significantly on the maximum pressure differential, although the zero venting design are more common for higher max ΔP
- The fuselage width is the parameter most impacting the mass of block fuel, much more than max ΔP. An increase in width of 1.5 m results in a 20-25% increase in block fuel, with a linear relation between fuselage width and block fuel (the cabin layout and length are however fixed in this analysis). The mass of the tank, its efficiency, or the mass of vented hydrogen don't seem to be affected a lot by this variable. The fuselage length starts to decrease when the fuselage width, i.e., tank radius, starts to increase, which is logical as its volume depends on its radius



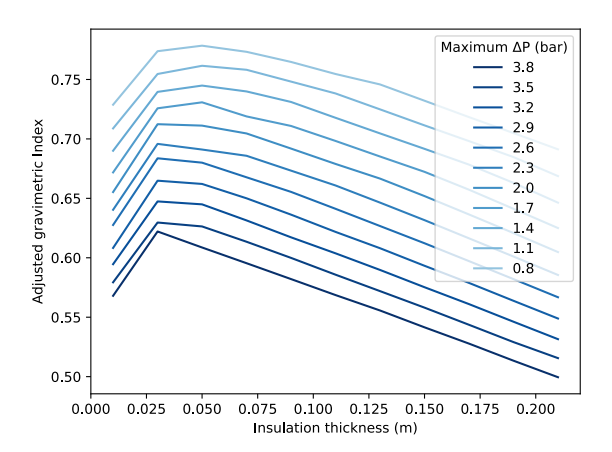


Figure 9 – Impact of maximal pressure differential and insulation thickness on tank efficiency

squared. However, this trend disappears quickly as the increase in block fuel leads to more storage volume required, meaning a longer tank and a longer fuselage.

- The amount of vented hydrogen decreases exponentially with the insulation thickness. With a very small insulation layer, the amount of unusable hydrogen can be very high (around 500kg with a 2 cm thick insulation layer), but this drops quickly. However, a very thick layer of 20 cm doesn't always prevent venting, probably when it is combined with a low max ΔP.
- The initial liquid temperature seems to have a small effect on the total amount of vented hydrogen, which is logical as a colder liquid will takes some time before it reaches saturation temperature. It also have a small impact on the fuselage, i.e the tank length as in this model the tank is sized with a hydrogen liquid density corresponding to the initial temperature.
- The transmission ratio of the shear loads have no visible effect on the aircraft and tank performance, or the effect is too small compared to the other parameters to distinguish. The bending transmission ratio might have a light impact on tank weight and efficiency, but it is one or two orders of magnitude lower.

With most gravimetric indexes above 0.5, it also suggests that hydrogen aircraft are feasible and should have comparable energy consumption to kerosene aircraft. This DOE clearly states nevertheless that some tank parameters have a significant impact on hydrogen aircraft performances and characteristics. The scale of this impact can vary significantly between parameters, so more in-depth parametric studies were conducted in the following section to quantify more precisely this dependency.

3.2 Parametric studies

3.2.1 Influence of tank insulation and design pressure

While designing a cryogenic hydrogen tank, two of the most important design variables are the insulation thickness and the maximum pressure differential the tank structure has to withstand. For both, increasing their value will reduce the hydrogen lost due to boiling and venting at the cost of added empty weight. To get some insight into this trade-off, a parametric study on those two variables was carried out. In this analysis, the same assumption as in the previous section 3.1 are made. The tank is fully integral, so the fuselage bending and shear loads are fully transmitted to the tank structure. The fuselage width is fixed at 4 m, similar to current medium-range aircraft like the A320 family.

Figure 9 illustrates how this trade-off affects tank performance. It can be observed that the amount of vented hydrogen during the mission can be significant for light insulation, with around 1 tons of hydrogen lost for 1 cm thick insulation. This loss decreases nevertheless exponentially with the thickness of the insulation, resulting in improved adjusted gravimetric indexes. The optimal insulation thickness to

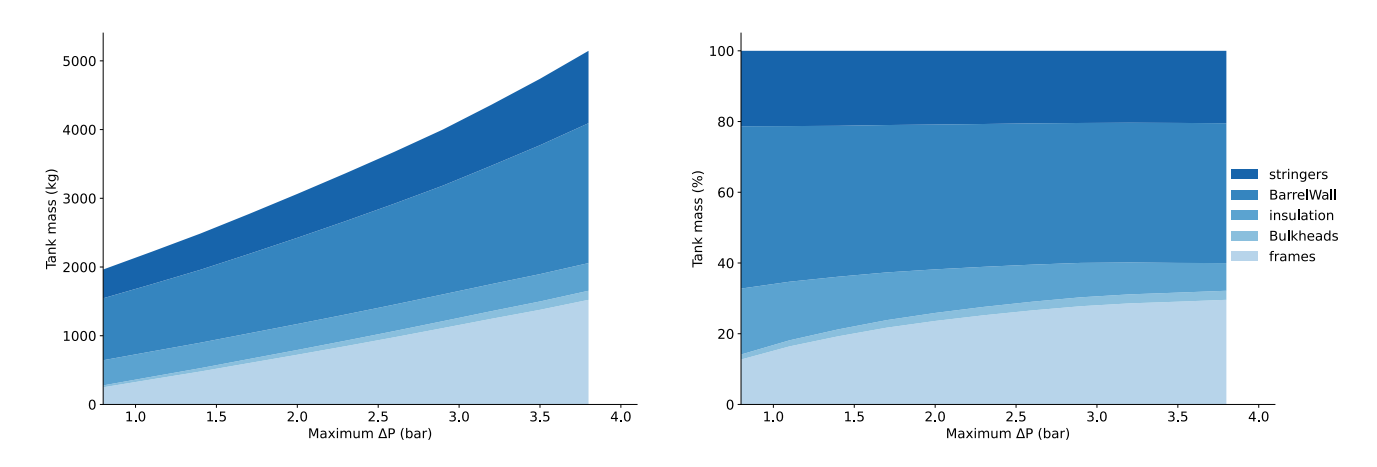


Figure 10 – Impact of maximal pressure differential on tank mass (insulation thickness fixed to 7 cm)

maximize the gravimetric index lies around 6-7 cm depending on the maximum ΔP , with an optimum ranging from 0.6 for high pressure to 0.78 for low pressure differential. This 20% wide range seems constant across all insulation thicknesses. Figure10 shows that total tank mass rises almost linearly with maximum ΔP for a 7 cm thick insulation, and the constant range mentioned previously indicates that it is the case for all insulation thicknesses. Figure10 confirms results already reported by the authors in [25], i.e., the significant contribution of the stiffening structure to the total tank mass. This contribution becomes even more important as the sizing pressure differential increases. It indeed represents around half of the mass when the maximum ΔP is above 3 bars.

Zero venting designs can be achieved with reasonable insulation thicknesses, for example 5 cm if the maximum ΔP is set above 2.5 bars 9. This threshold is harder to reach with a lower maximum ΔP , with at least 10 to 12cm required if $\Delta P=1$ bar. It should finally be noted that if the configuration is not a zero-venting design, the sensitivity of hydrogen boil-off to insulation thickness is very strong. The amount of hydrogen lost can so quickly represent a non-negligible block fuel percentage. Correctly identifying the optimum insulation thickness is therefore absolutely necessary, and comfortable safety margins should be introduced. A longer dormancy phase after landing could also lead to a higher amount of hydrogen being vented. If venting is prohibited during that phase, it could set severe constraints on insulation thickness, as presented in Section 3.2.5

3.2.2 Influence of fuselage width for integral tanks configurations

According the DOE presented in Figure 8, if tank characteristics like insulation thickness and design pressure strongly impact its performance, the fuselage width has the biggest impact on aircraft efficiency. To understand this phenomenon more in detail, a parametric study on this parameter was conducted. The same design hypotheses are made so the tank is still integral, i.e., its diameter is equal to the fuselage width, and 7 cm of insulation are placed inside the tank. Figure 11 shows the evolution of the block fuel and the tank mass with respect to the fuselage diameter for different values of the maximum design pressure differential. As expected, on the left graph, block fuel increases significantly with fuselage width (approximately +10%/m). This is true for all maximum design pressure differential.

The right graph in Figure 11 illustrates that fuselage diameter has only a small impact on tank mass, especially at low design pressure. Increasing the tank radius will indeed increase the stress in the wall and stiffening structure, as it depends on the radius. It results in a thicker wall and a bigger frame section, as the stress depends on that radius. But it also increases the volume-to-external surface ratio, meaning that less wall surface is needed, diminishes the stress due to the bending moment and reduces the tank length, requiring shorter stringers and maybe fewer frames. This explains why the mass of the tank can even decrease a little when the tank radius grows 12.

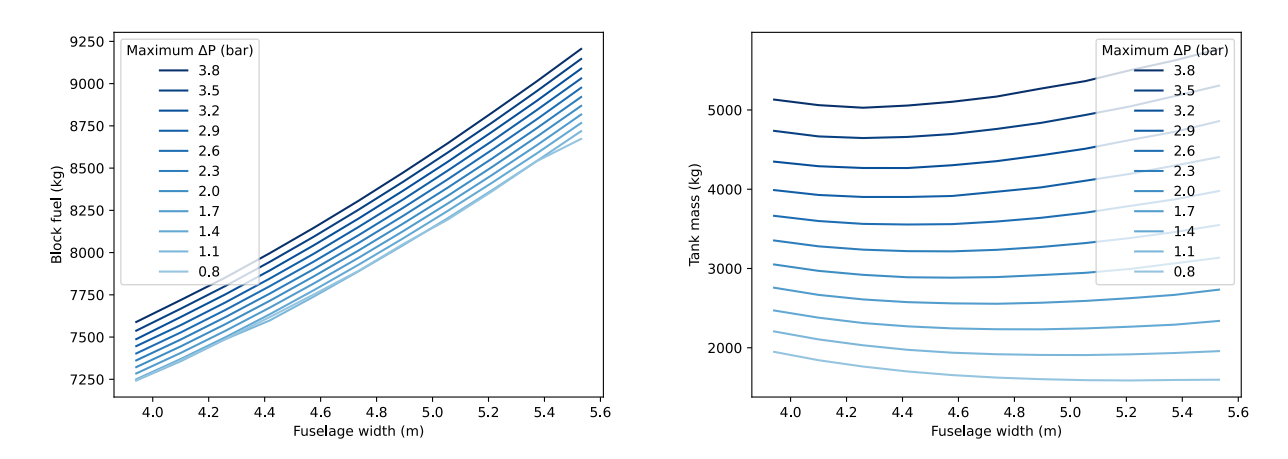


Figure 11 - Evolution of aircraft consumption and tank mass with fuselage width

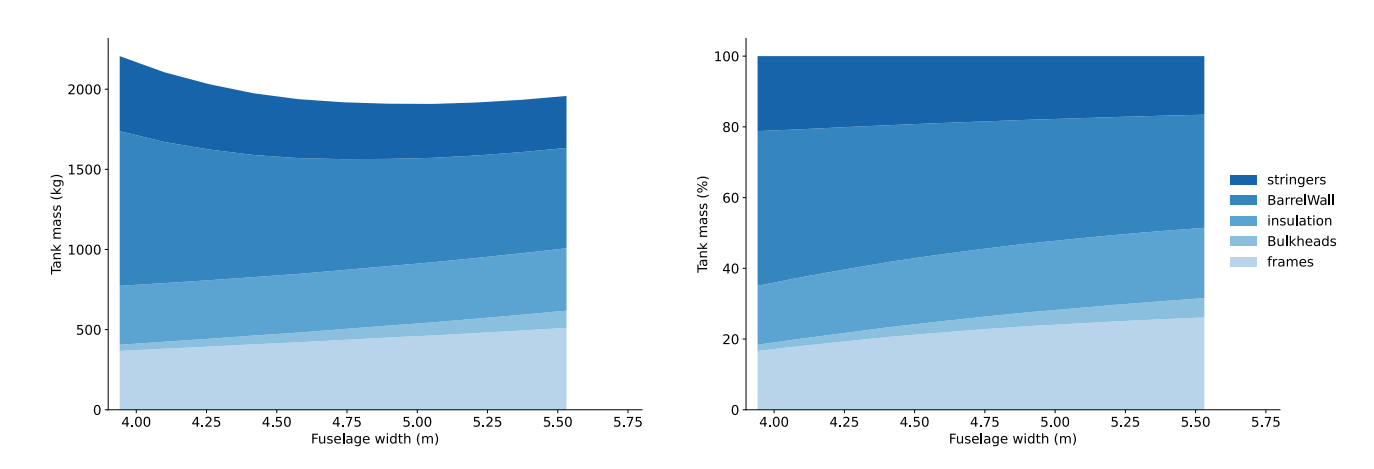
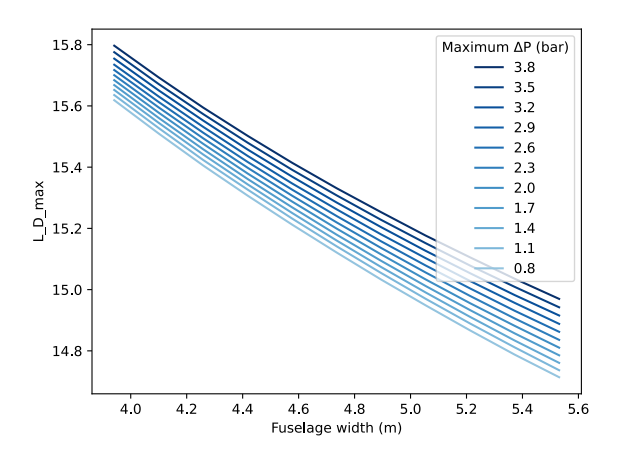


Figure 12 – Impact of fuselage radius on integral tank mass (max ΔP fixed to 1.1 bar)



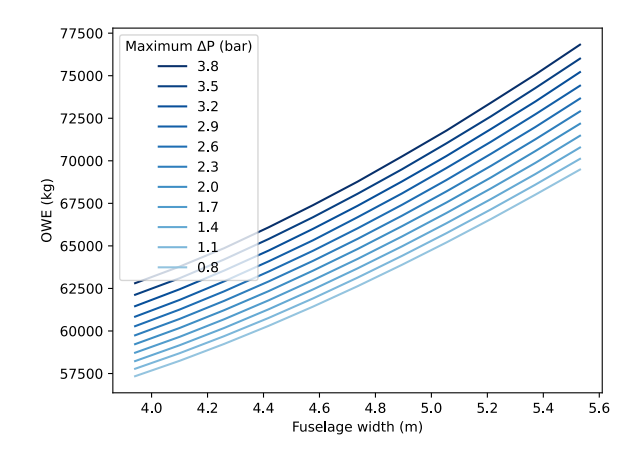


Figure 13 – Impact of fuselage width on aircraft operational empty weight and lift-to-drag ratio

If the tank mass stays almost constant when the fuselage width increases, the rise in aircraft consumption comes logically from other factors. After a deeper analysis, two contributions arise: a heavier fuselage and a bigger wetted surface, resulting in more drag. The impact on those two contributions can be seen in Figure 13: by increasing the fuselage diameter by 1.5 m, the empty weight of the aircraft can rise by 15 to 20% depending on the maximum design pressure. The lift-to-drag ratio is also reduced by approximately 4-5%, which explains the rise in fuel consumption. Those results are, however, probably overestimating this increased consumption as the length of the fuselage is not reduced (the cabin layout remains a single aisle with 6 seats (3–3) per row across the whole study). The semi-empirical relations used to determine fuselage mass were also created for single-aisle, aluminum fuselages. New wide-body fuselages are made from composite material, which significantly reduces their mass.

To confirm the strong impact of the fuselage radius on aircraft efficiency, another analysis was conducted. Three twin-aisle aircraft with different cabin layouts were modeled and compared to a reference single-aisle aircraft. The selected cabin layouts are 7 passengers per row, distributed as 2-3-2 seats, 9 passengers per row (3-3-3) and 10 passengers per row (3-4-3). Unlike the previous analysis, this time the cabin length is optimized according to the number of seat rows it must contain. The evolution of aircraft characteristics with each cabin layout compared to the reference aircraft is presented in Figure 14. As expected, the block fuel rises significantly for larger fuselages compared to a single-aisle, with a maximum increase of 18% for the 10 seats per row cabin layout. This is due to the augmentation of the empty weight as well as the degradation of the aerodynamic efficiency. Wider fuselages are indeed shorter, but they still represent a bigger wetted area, resulting in a bigger mass and more friction drag. Even the tendency of the hydrogen tank to maintain an almost constant gravimetric index doesn't compensate for the disadvantage of a bigger fuselage.

3.2.3 Integral and non-integral tank trade-off

In previous analysis, modeled tanks were all considered integral tanks, where the entire fuselage bending and shear load is transmitted to the tank. However, some hydrogen aircraft design present a non-integral tank, which is placed inside the fuselage. This allows for easier insulation, as it can placed on the external surface, and easier integration into current aircraft designs. Some drawbacks of this configuration are the more complex access to the tank for inspection or repairs and the added weight of the fuselage surrounding the tank. The transmission of fuselage bending and shear loads will also depend on the tank's attaching structure. As this structure is not modeled into the current FAST-OAD version, a parametric study was made to determine how much those loads can affect the tank design. In this analysis, the insulation thickness was fixed to 7 cm and the maximum design pressure differential was set at 1 bar.

Figure 15 shows the evolution of tank gravimetric efficiency and block fuel with the proportions of

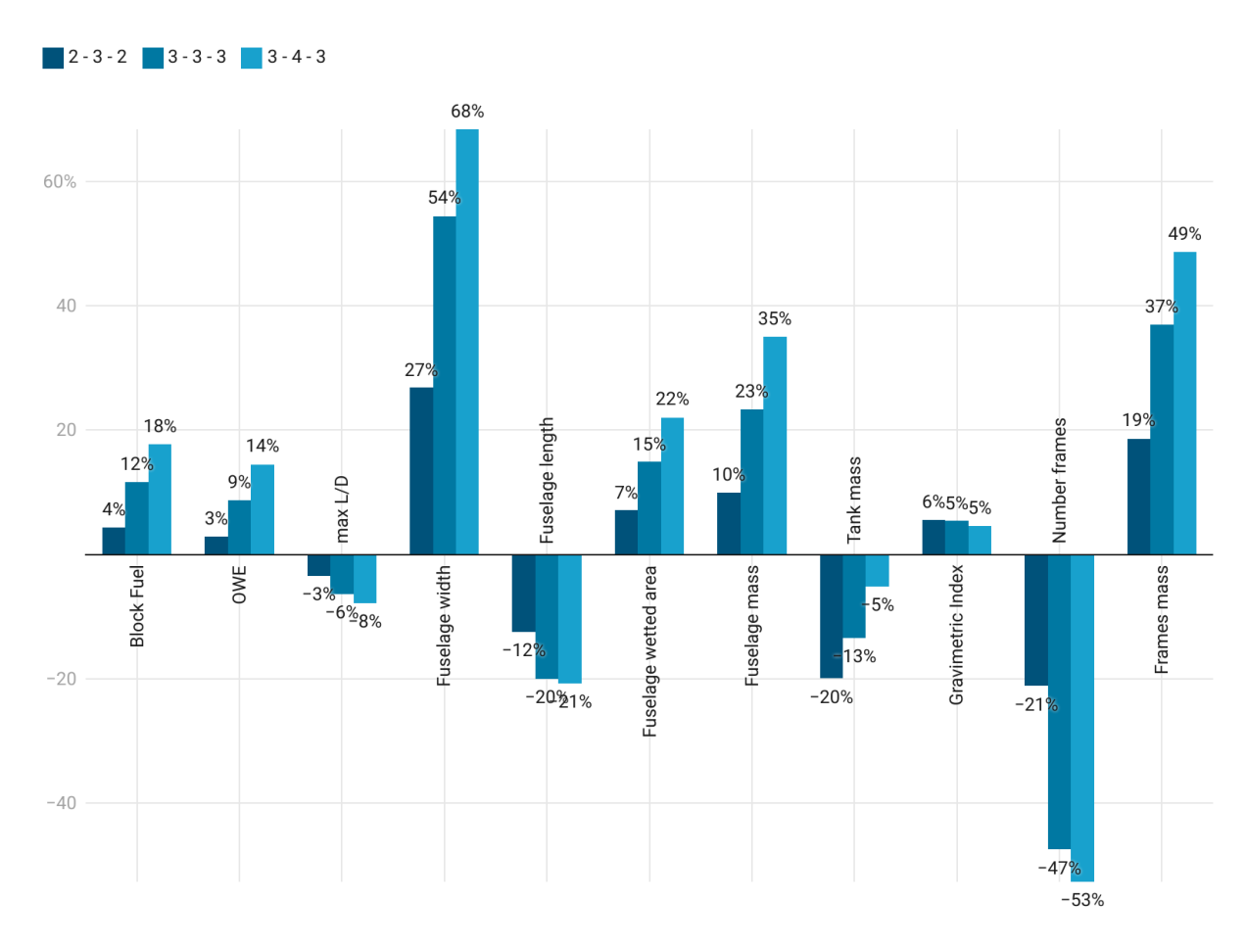


Figure 14 – Evolution of hydrogen aircraft characteristics and performance of twin-aisle cabin configurations compared to a single-aisle

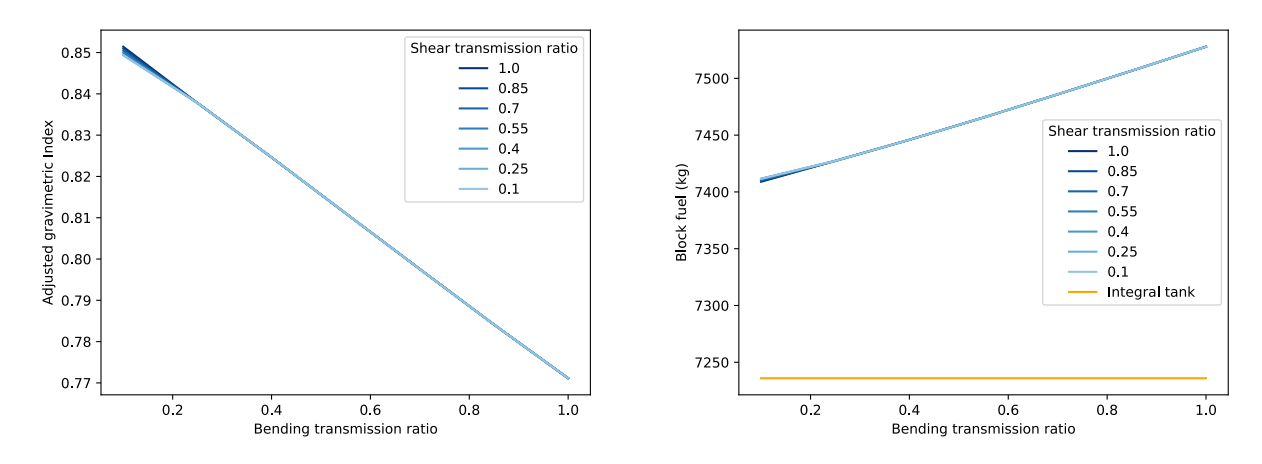


Figure 15 - Impact of fuselage loads transmission to the tank on aircraft performance

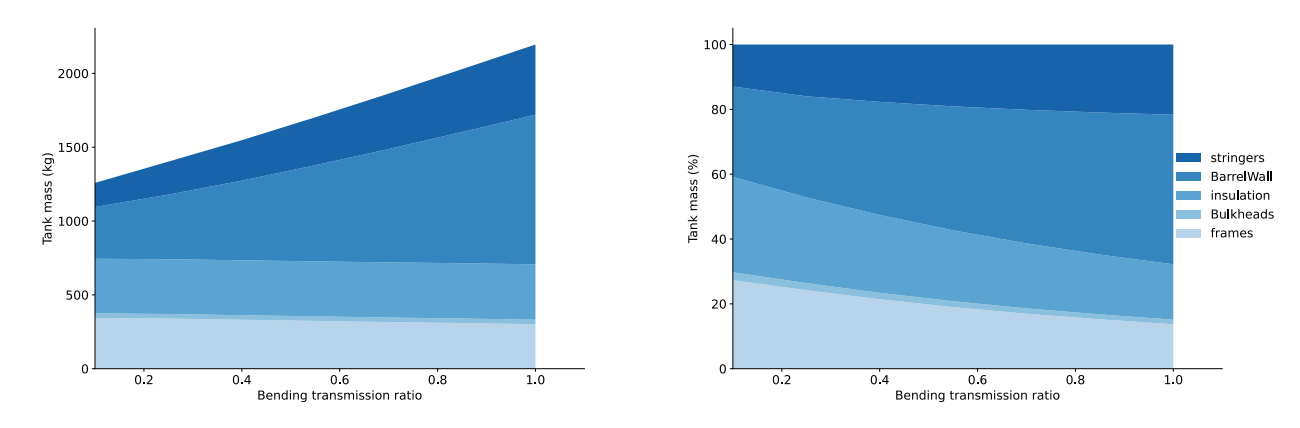


Figure 16 – Impact of fuselage loads transmission on hydrogen tank mass

the fuselage's shear and bending loads that are transmitted to the tank. The shear load impact is negligible on the tank design, having a visible effect only for low bending load transmissions ratio, although the effect remains small. However, the bending moment can significantly affect the tank. Figure 16 illustrates indeed how a tank that must fully withstand the bending moment of the fuselage can be around 70% heavier than a tank that is lightly loaded. This is due mainly to the increase in tank wall and stringer mass: their contribution to total tank mass almost doubles when the load transmission ratio goes from 0.1 to 1. It results in a gravimetric efficiency index that drops by 0.08, explaining the higher block fuel.

These results seem to suggest that a non-integral tank can offer better performance if a limited amount of bending load is transmitted to it. But as the structure to fix such a tank into a fuselage was not considered in this analysis, further investigations are needed to assess how much the added weight of this system would reduce this advantage. In any case, the fuel efficiency of hydrogen aircraft with a non-integral tank appears to be always 2% to 4% above that of an integral tank design, even without considering the structure to attach a non-integral tank. This is due to the weight penalty of having a fuselage around the tank.

3.2.4 Influence of design range hydrogen aircraft efficiency

In recent history, improvements in aircraft engine-specific consumption have often resulted in increased maximum range for each new aircraft generation. The reason for this can be seen in figure 17 on the left graph, where the energy consumption of a kerosene aircraft increase linearly with the design range. This means that increasing the design range for jet-A-fueled aircraft doesn't significantly affect the average fuel consumption per nautical mile. Unlike conventional aircraft however, the average energy consumption of hydrogen aircraft seems more dependent on their design range past 2000 NM.

This can be linked to the hydrogen tank gravimetric index quickly dropping after 1700 NM in Figure 17. As more fuel is needed for the mission, the hydrogen tank becomes indeed longer. This deteriorates its surface-to-volume ratio, leading to a lower thermal efficiency and a higher empty mass-to-volume ratio, which explains the evolution of the gravimetric index. It also necessitates a longer fuselage, generating more friction drag, something that doesn't affect kerosene aircraft, which can easily store fuel in its wing up to 3000NM.

Those reasons explain the difference in energy consumption between conventional and hydrogen aircraft. Between 1000 NM and 2000 NM, this difference decreases from 9% to 7%, probably because the tank performance is stable. After 2000 NM design range, it grows wider again, such that hydrogen aircraft consume 10% more energy at 2500 NM and 12% at 3000 NM.

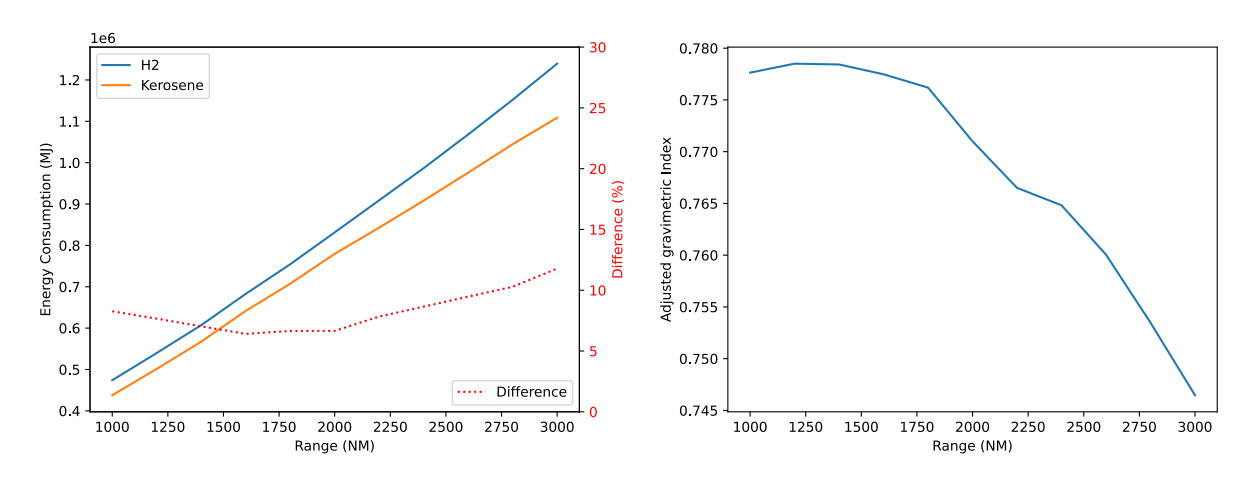


Figure 17 – Evolution of aircraft energy consumption and tank efficiency with design range

3.2.5 Influence of a zero venting constraint during dormancy phase

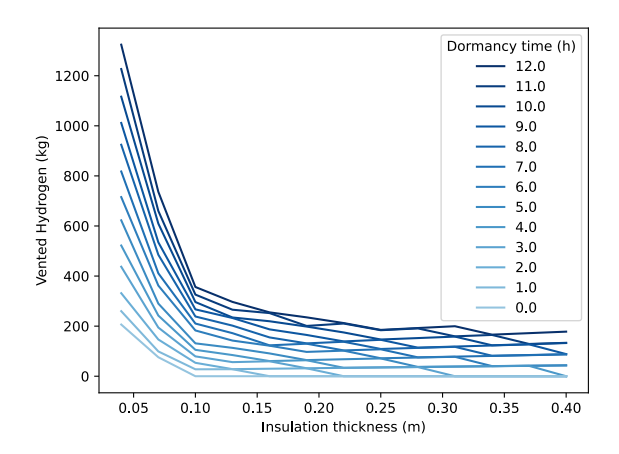
With the current air transport organization, aircraft can spend several hours at the airport between two flights. During the night, they can stay up to 12 hours parked on the runway. This time is called the dormancy time, and some airlines have expressed concerns about the safety constraints of hydrogen aircraft during that phase. Safety regulations might indeed forbid all potential venting of hydrogen on the ground to avoid a fire or an explosion. Therefore, a trade-off analysis is necessary to assess the feasibility of a hydrogen aircraft design that eliminates the need for venting during dormancy.

Figure 18 shows the results of a sensitivity analysis where the insulation thickness and the dormancy time varied between respectively from 4 to 40 cm, and from 0 to 12 hours. The sensitivity to the maximum design pressure differential was not analyzed (it was fixed to 1 bar), as previous analysis demonstrated the better trade-off of improving the insulation.

Results show above all that a long dormancy phase will significantly increase the block fuel. This is due to ever lots of hydrogen will being vented for low insulation thickness, or because of the volume and weight of very thick insulation deteriorate aircraft performance. The mass of the empty tank is indeed multiplied by 4 between a 5cm and 40 cm thick insulation (half of it due to the insulation weight and half to the longer tank required). With the current model, even a 40cm thick insulation is insufficient to have a zero venting dormancy of more than 7 hours. With a more reasonable 20 cm thick insulation, a dormancy time of around 2 hours can be achieved at the cost of a small degradation of the block fuel. Those results suggest that the constraint of zero venting during dormancy is extremely impactfull and should be reduced if possible. Alternative solution like connecting the aircraft to the fuel distribution system where it could vent hydrogen gas could be more economically interesting. Otherwise more efficient insulation technologies like multi-layer or vacuum insulation should be used, but with a probable high impact on the tank weight.

4. Conclusion

This work capitalized on the hydrogen tank sizing methodology previously developed by the authors by integrating it into the aircraft design tool FAST-OAD. The structural sizing of the tank was added to the aircraft's overall structure design, while the mission module is now post-processed by the thermodynamic model to estimate the amount of hydrogen vented during a mission. The hydrogen aircraft design framework created was used to conduct parametric studies in order to assess the impact of tank and mission parameters on aircraft performance. The major impact on aircraft efficiency seems to be the fuselage radius, which also determines the tank radius. In this regard, wider fuselage always resulted in lower global performance due to their bigger surface, which led to a heavier structure and higher drag. The characteristics of the hydrogen tank also depend on its radius, but its gravimetric index remains nearly constant as different factors balance each other out. The adjusted gravimetric index is however strongly affected by the maximum pressure differential between the tank interior and exterior. A high maximum design pressure can therefore negatively affect fuel consumption. The



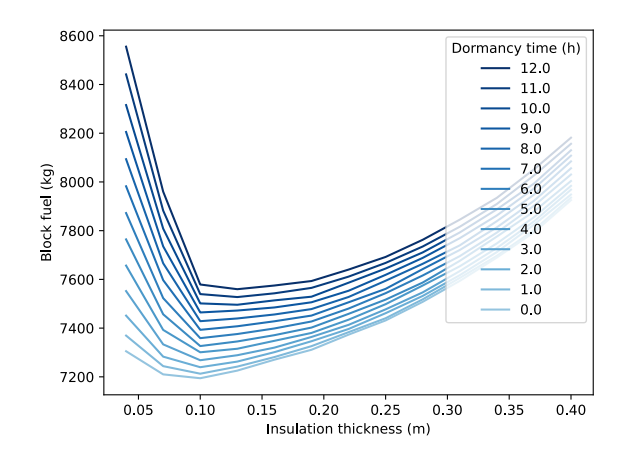


Figure 18

insulation can also have a major impact, but the amount of hydrogen to be vented during a mission decreases exponentially with its thickness and a zero-venting design can be achieved. Concerning non-integral tank, fuel consumption always appears to be a few percent higher than integral design. The exact increase depends on the proportion of bending moment that is transmitted from the fuse-lage to the tank, ranging from 2% to 4%. The best tank configuration seems therefore to be a integral tank with a maximum design pressure of 1 bar to 1.5 bar and an insulation thickness of 7–10 cm for a low-venting design. A zero-venting policy during the dormancy period could nevertheless require a thicker insulation, but it would mean a significant deterioration of the fuel efficiency for periods above 2 hours. In the end, the best identified medium range hydrogen aircraft configuration would consume approximately 10% more energy than conventional kerosene aircraft, while still having the benefit of zero CO2 emission in flight.

5. Contact Author Email Address

mailto: romain.parello@onera.fr

6. Copyright Statement

The authors confirm that they, and/or their company or organization, hold copyright on all of the original material included in this paper. The authors also confirm that they have obtained permission from the copyright holder of any third-party material included in this paper to publish it as part of their paper. The authors confirm that they give permission, or have obtained permission from the copyright holder of this paper, for the publication and distribution of this paper as part of the ICAS proceedings or as individual off-prints from the proceedings.

References

- [1] V. Masson-Delmotte, P. Zhai, A. Pirani, S.L. Connors, C. Péan, S. Berger, N. Caud, Y. Chen, L. Goldfarb, M.I. Gomis, M. Huang, K. Leitzell, E. Lonnoy, J.B.R. Matthews, T.K Maycock, T. Waterfield, O. Yelekçi, R. Yu, and B. Zhou. Climate Change 2021: The Physical Science Basis. Contribution of Working Group I to the Sixth Assessment Report of the Intergovernmental Panel on Climate Change. Technical report, Cambridge University Press, 2021.
- [2] D. S. Lee, D. W. Fahey, A. Skowron, M. R. Allen, U. Burkhardt, Q. Chen, S. J. Doherty, S. Freeman, P. M. Forster, J. Fuglestvedt, A. Gettelman, R. R. De León, L. L. Lim, M. T. Lund, R. J. Millar, B. Owen, J. E. Penner, G. Pitari, M. J. Prather, R. Sausen, and L. J. Wilcox. The contribution of global aviation to anthropogenic climate forcing for 2000 to 2018. *Atmospheric Environment*, 244:117834, January 2021.
- [3] Joseph Brand, Sam Sampath, Frank Shum, Robert Bayt, and Jeffrey Cohen. Potential Use of Hydrogen In Air Propulsion. In *AIAA International Air and Space Symposium and Exposition: The Next 100 Years*, Dayton, Ohio, July 2003. American Institute of Aeronautics and Astronautics.
- [4] David I. Barton, Cesare A. Hall, and Matthew K. Oldfield. Design of a Hydrogen Aircraft for Zero Persistent Contrails. *Aerospace*, 10(8):688, August 2023. Number: 8 Publisher: Multidisciplinary Digital Publishing Institute.

Integrating Cryogenic Tanks Model in Hydrogen Aircraft Design for Parametric Performance Analysis

- [5] G. Daniel Brewer. Hydrogen Aircraft Technology. Routledge, New York, 1 edition, 1991.
- [6] A. Westenberger. Liquid Hydrogen Fuelled Aircraft System Analysis (CRYOPLANE). Technical, Airbus Deutschland GmbH, September 2003.
- [7] Fuel Cells and Hydrogen 2 Joint Undertaking (EU body or agency) Now known as... *Hydrogen-powered* aviation: a fact based study of hydrogen technology, economics, and climate impact by 2050. Publications Office of the European Union, 2020.
- [8] Vittorio Cipolla, Davide Zanetti, Karim Abu Salem, Vincenzo Binante, and Giuseppe Palaia. A Parametric Approach for Conceptual Integration and Performance Studies of Liquid Hydrogen Short–Medium Range Aircraft. *Applied Sciences*, 12(14):6857, January 2022. Number: 14 Publisher: Multidisciplinary Digital Publishing Institute.
- [9] Giuseppe Palaia, Karim Abu Salem, and Erasmo Carrera. Preliminary Performance Analysis of Medium-Range Liquid Hydrogen-Powered Box-Wing Aircraft. *Aerospace*, 11(5):379, May 2024. Number: 5 Publisher: Multidisciplinary Digital Publishing Institute.
- [10] C.W.C Van Woensel. Integration of a Liquid Hydrogen Fuel Tank into the Concept of the Flying-V. Master's thesis, TU Delft, June 2021.
- [11] Raúl Quibén Figueroa, Rauno Cavallaro, Andrea Cini, and Manuel Soler Arnedo. *MOTIVATION (Mdao fOr susTalnable aViATION)* Framework development for the design and optimization of H2 powered aircraft. In *AIAA AVIATION 2023 Forum*, San Diego, CA and Online, June 2023. American Institute of Aeronautics and Astronautics.
- [12] Marc Prewitz, Jonas Schwärzer, and Andreas Bardenhagen. Potential analysis of hydrogen storage systems in aircraft design. *International Journal of Hydrogen Energy*, 48(65):25538–25548, July 2023.
- [13] David Maniaci. Relative Performance of a Liquid Hydrogen-Fueled Commercial Transport. In *46th AIAA Aerospace Sciences Meeting and Exhibit*, Reno, Nevada, January 2008. American Institute of Aeronautics and Astronautics.
- [14] Eytan J Adler and Joaquim R. R. A. Martins. Hydrogen-Powered Aircraft: Fundamental Concepts, Key Technologies, and Environmental Impacts. *Progress in Aerospace Sciences*, 2023.
- [15] Jon Huete and Pericles Pilidis. Parametric study on tank integration for hydrogen civil aviation propulsion. *International Journal of Hydrogen Energy*, 46(74):37049–37062, October 2021.
- [16] Swapnil S. Jagtap, Peter R. N. Childs, and Marc E. J. Stettler. Performance sensitivity of subsonic liquid hydrogen long-range tube-wing aircraft to technology developments. *International Journal of Hydrogen Energy*, 50:820–833, January 2024.
- [17] Dries Verstraete. *The Potential of Liquid Hydrogen for long range aircraft propulsion*. PhD thesis, Crandfield, April 2009.
- [18] Christopher Winnefeld, Thomas Kadyk, Boris Bensmann, Ulrike Krewer, and Richard Hanke-Rauschenbach. Modelling and Designing Cryogenic Hydrogen Tanks for Future Aircraft Applications. *Energies*, 11(1):105, January 2018. Number: 1 Publisher: Multidisciplinary Digital Publishing Institute.
- [19] Paulas Raja Sekaran, Amir S. Gohardani, Georgios Doulgeris, and Riti Singh. Liquid hydrogen tank considerations for turboelectric distributed propulsion. *Aircraft Engineering and Aerospace Technology*, 86(1):67–75, December 2013.
- [20] Arturo Gomez and Howard Smith. Liquid hydrogen fuel tanks for commercial aviation: Structural sizing and stress analysis. *Aerospace Science and Technology*, 95:105438, December 2019.
- [21] D Silberhorn, G Atanasov, J-N Walther, and T Zill. Assessment of hydrogen Fuel Tank Integration at Aircraft Level. German Aerospace Center (DLR), Hamburg, September 2019.
- [22] L G Bolshinskiy, A Hedayat, L J Hastings, and J P Moder. Tank System Integrated Model: A Cryogenic Tank Performance Prediction Program. Technical Memorandum, NASA, Marshall Space Flight Center, Huntsville, Alabama, April 2017.
- [23] G. Onorato, P. Proesmans, and M. F. M. Hoogreef. Assessment of hydrogen transport aircraft: Effects of fuel tank integration. *CEAS Aeronautical Journal*, 13(4):813–845, October 2022.
- [24] Romain Parello, Sebastien Defoort, Emmanuel Benard, and Yves Gourinat. Design and Integration of a Liquid Hydrogen Tank on an Aircraft. In *AIAA SCITECH 2024 Forum*, Orlando, FL, January 2024. American Institute of Aeronautics and Astronautics.
- [25] R Parello, Y Gourinat, E Benard, and S Defoort. Structural sizing of a hydrogen tank for a commercial aircraft. *Journal of Physics: Conference Series*, 2716(1):012040, March 2024.
- [26] Christophe David, Scott Delbecq, Sebastien Defoort, Peter Schmollgruber, Emmanuel Benard, and Valerie Pommier-Budinger. From FAST to FAST-OAD: An open source framework for rapid Overall Aircraft Design. *IOP Conference Series: Materials Science and Engineering*, 1024(1):012062, January 2021.
- [27] Certification Specifications and Acceptable Means of Compliance for Large Aeroplanes (CS-25), Novem-

ber 2021.

- [28] Justin S. Gray, John T. Hwang, Joaquim R. R. A. Martins, Kenneth T. Moore, and Bret A. Naylor. OpenM-DAO: an open-source framework for multidisciplinary design, analysis, and optimization. *Structural and Multidisciplinary Optimization*, 59(4):1075–1104, April 2019.
- [29] Elodie Roux. *Modèles Moteur . . . Réacteurs double flux civils et réacteurs militaires à faible taux de dilution avec PC*. PhD thesis, Toulouse, France, 2002.
- [30] AIRBUS S.A.S. A321 AIRCRAFT CHARACTERISTICS : AIRPORT AND MAINTENANCE PLANNING, 2005.
- [31] David B. Fenn, Loren W. Acker, and Joseph S. Algranti. Flight Operation of a Pump-Fed Liquid-Hydrogen Fuel System. Technical Report NASA-TM-X-252, April 1960. NTRS Author Affiliations: NASA Lewis Research Center NTRS Document ID: 19680068699 NTRS Research Center: Glenn Research Center (GRC).
- [32] Yves GOURINAT. Charges structurales en vol Dimensionnement de panneaux fuselage. *Techniques de l'ingénieur: Systèmes aéronautiques et spatiaux*, (TRP 4033 V1), August 2017. Editions T.I.
- [33] Ian H. Bell, Jorrit Wronski, Sylvain Quoilin, and Vincent Lemort. Pure and Pseudo-pure Fluid Thermophysical Property Evaluation and the Open-Source Thermophysical Property Library CoolProp. *Industrial* & Engineering Chemistry Research, 53(6):2498–2508, February 2014. Publisher: American Chemical Society.
- [34] Mingxuan Shi, Imon Chakraborty, Jimmy C. Tai, and Dimitri N. Mavris. Integrated Gas Turbine and Environmental Control System Pack Sizing and Analysis. In *2018 AIAA Aerospace Sciences Meeting*, Kissimmee, Florida, January 2018. American Institute of Aeronautics and Astronautics.
- [35] Eugina Mendez Ramos. Enabling Conceptual Design and Analysis of Cryogenic In-Space Vehicles through the Development of an Extensible Boil-Off Model. PhD thesis, Georgia Institute of Technology, ATLANTA, US, May 2021.